Mobile arm for disabled people assistance Manipulability measure for redundancy solve

KHIAR NAIT-CHABANE, PHILIPPE HOPPENOT, ETIENNE COLLE

Complex System Laboratory (LSC), University of Evry, France

http://lsc.univ-evry.fr

E mail: chabane@iup.univ-evry.fr
Tel : (33/0) 1 69 47 75 04
Fax : (33/0) 1 69 47 06 03

Abstract

The addition of a mobile platform to a 6-DOF arm raises the question of the exploitation of redundancy with respect to needs. The application field concerns assistive robotics for object manipulation tasks. Works deal with the utilisability of a mobile arm, which is a complex system, by a disabled person with reduced motor and perception abilities.

In this paper, we present the influence of mobility on manipulability measure. Manipulability is a well-established tool for motion analysis which we use as criterion in control scheme to improve the coordination of two subsystems. We propose a normalized measure to solve problems inherent to the use of different physical units and velocity limits for both components of the system, arm and mobile platform. Simulation results for a 3D positioning task are given to show the effect of nonholonomic constraint on manipulability measure.

Key Words: Robotized assistant, mobile manipulator, nonholonomic systems, manipulability

Abbreviations: EE, End-effector; DOF, Degre of Freedom

1. Introduction

Tele-operation covers a large spectrum of situations. In all these situations, a human operator pilots a distant machine through an adequate interface. Figure1 illustrates a remote control situation.

In rehabilitation robotics, the challenge is to put in adequacy the control of a complex machine with the limited capacities of a handicapped person. The main assistance offers by ARPH (Assistant Robot for People with Handicap) is for object manipulation by upper limb disabled people with or without mobility. The system is composed of a manipulator arm mounted on a mobile base and can be remotely controlled (figure.1).

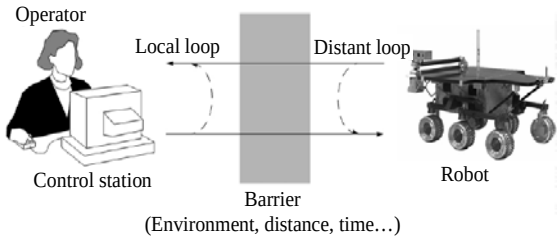

Figure 1: Remote control situation (adapted from (Fong, 2001)).

Laboratory previous works dealt with human machine cooperation for controlling the displacement of the robot in another part of the residence. Three kinds of control modes have been proposed. In the manual mode, the person directly pilots the robot through the control station and an adequate man-machine interface. In the opposite, in the automatic mode, the operator only chooses the goal and the robot achieves the mission alone (Rybarczyck et al., 2002). Shared mode concept seems more interesting. In that case, human operator and machine co-operate to achieve the mission. For example, it is possible for the user to pilot the displacement of the mobile base as in manual mode but with a security given by obstacle avoidance, automatic task realised by the robot. The major difficulty met by an operator who acts on a semi-automatic system is to take the control back, because he generally does not understand how the system works during the automatic step. Inversely, our assumption is that, if the robot acts “as a human being", the operator would better understand its behaviour and then control it more easily. (Rybarczyck et al., 2001), (Mestre, 2005) have shown an enhancement of performance of man-machine co-operation for navigation tasks in

this case. Laboratory current works deal with the control of the whole mobile arm for object grasping. The same approach as for navigation tasks is followed but for giving human like behaviour for grasping. We search to privilege manipulability by using the system redundancy while minimizing acceleration variations and smoothing trajectories for EE movements. It is typically a human-like behavior which allows the reduction of expenditure of energy (Alexander, 1997).
The paper is organized as follows. In section 2, we present the modeling of the mechanical system. Firstly we introduce arm modeling, platform modeling and then whole system modeling. Manipulability concept of manipulator arms and its extension to the case of mobile manipulators is studied in section 3. Different measures of manipulability and their normalisation are given in the same section. Section 4 reports and discusses simulation results on manipulability. First, we analyse the manipulability measures of manipulator then the whole system for positioning tasks. Finally, the arm manipulability is used in a global control scheme.

2. Modeling of the Robotized Assistant

The mobile manipulator used in *ARPH* project (Hoppenot, 2002) consists of a Manus arm manufactured by Exact Dynamics Company, mounted on a mobile platform powered by two independent drive wheels (figure 2).

Figure 2: ARPH system

Let us define a fixed world frame of reference $\{W\}$, a moving platform frame $\{P\}$ attached to the middle of the two drive wheels, a moving arm frame $\{A\}$ related to the manipulator base and a moving end-effector frame $\{E\}$ attached to the arm end-effector (figure 3).

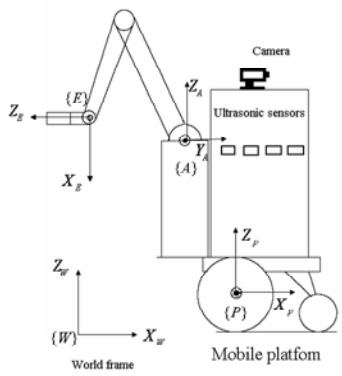

Figure 3: Mobile manipulator system

We adopt the following assumptions in modeling the mobile manipulator system. There is no slipping between the wheel and the floor. The platform can not move sidelong to maintain the nonholonomic constraint. The manipulator is rigidly mounted on the platform.

2.1 Manipulator arm modeling

The forward kinematics of a serial chain manipulator that relates the joint space and the task space variables is expressed by:

$$X_a = f_a(q_a) \tag{1}$$

where $X_a = [x_{a1}, x_{a2}, \cdots x_{am}]^T \in R^m$ is the vector of the task variables in *m*-dimensional task space, $q_a = [q_{a1}, q_{a2}, \cdots q_{an}]^T \in R^n$ is the vector of joint variables in the *n*-dimensional variables, called generalized coordinates, and f_a is the nonlinear function of the forward kinematic mapping.

Differentiating equation (1) with respect to time, we obtain a linear equation in velocity level:

$$\dot{X}_a = J_a(q_a)\dot{q}_a \tag{2}$$

where $\dot{X}_a$ is the task velocity vector, $\dot{q}_a$ is the joint velocity vector, and $J_a(q_a)$ is Jacobian matrix.

For kinematic modeling of the considered manipulator arm, we use the Denavit Hartenberg parameters (Sciavicco, 1996). Manus arm has six rotoide joints, with 3DOF for gripper positioning and 3DOF for gripper orientation. The Cartesian coordinates of the end-effector relative to the arm base frame {*A*} are given by

$$X_a = \begin{cases} x_{a1} = (L_4 c_3 + L_3 c_2) c_1 - L_2 s_1 \\ x_{a2} = (L_4 c_3 + L_3 c_2) s_1 + L_2 c_1 \\ x_{a3} = L_4 s_3 + L_3 s_2 \\ x_{a4} = \phi \\ x_{a5} = \theta \\ x_{a6} = \psi \end{cases} \quad (3)$$

where $c_i = \cos(q_{ai})$, $s_i = \sin(q_{ai})$ and L_2, L_3, L_4 represent respectively the length of arm links.

$[x_{a1}, x_{a2}, x_{a3}]^T$ and $[\phi, \theta, \psi]^T$ represent respectively the Cartesian coordinates and Euler angles of EE (Yoshikawa, 1990).

In this paper, we consider only the main three joints of the arm, corresponding to gripper positioning, given by the generalized coordinates vector $q_a = [q_{a1}, q_{a2}, q_{a3}]^T$.

2.2. Mobile platform modeling

The location of the platform is given by three operational coordinates x_p, y_p and θ_p defining its position and orientation as shown in figure 4.

Therefore, the generalized coordinates vector is $q_p = [x_p, y_p, \theta_p]^T$. Thus, the generalized velocities vector is $\dot{q}_p = [\dot{x}_p, \dot{y}_p, \dot{\theta}_p]$.

The nonholonomic constraint to which the platform is subjected has the following form:

$$A(q_p)\dot{q}_p = 0 \quad (4)$$

where $A(q_p) = [\sin(\theta_p) \ -\cos(\theta_p) \ 0]$.

The kinematic model of the mobile platform is given by (Bayle et al., 2001a):

$$\dot{q}_p = \begin{bmatrix} \cos(\theta_p) & 0 \\ \sin(\theta_p) & 0 \\ 0 & 1 \end{bmatrix} \begin{bmatrix} v \\ \omega \end{bmatrix} = S(q_p) u_P \quad (5)$$

where $u_p = [v, \omega]^T$. v and ω are the linear and angular velocities of the platform, respectively.

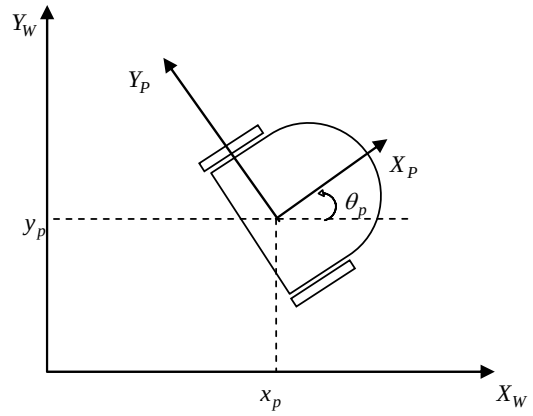

Figure 4: Wheeled mobile platform

2.3. Mobile manipulator modeling

The forward kinematic model of the mobile manipulator may be expressed in the following form (Seraji. 93):

$$X = f(q_p,\ q_a) \tag{6}$$

where q_p is the generalized coordinates of the mobile platform and q_a represents joint variables of the arm defined above.

Thus, the configuration of the mobile manipulator is defined by the *N* generalized coordinates (*N*=*n*+*3*):

$$q = [q_p^T, q_a^T]^T = [x_p, y_p, \theta_p, q_{a1}, \cdots, q_{an}]^T$$

The direct kinematic model for the positioning task of the considering mobile arm relative to world frame {*W*} is given by:

$$X = [x_1, x_2, \cdots, x_6]^T = f(q_a, q_p) \tag{7}$$

$$X = \begin{cases} x_1 = x_p + (x_{a2} + a)\cos(\theta_p) - (b - x_{a1})\sin(\theta_p) \\ x_2 = y_p + (x_{a2} + a)\sin(\theta_p) + (b - x_{a1})\cos(\theta_p) \\ x_3 = x_{a3} + c \\ x_4 = x_{a4} + \theta_p - \dfrac{\pi}{2} = \phi + \theta_p - \dfrac{\pi}{2} \\ x_5 = x_{a5} = \theta \\ x_6 = x_{a6} = \psi \end{cases} \tag{8}$$

where *a*, *b* and *c* are the Cartesian coordinates of the base manipulator arm with respect to the mobile platform frame {*P*}.

The instantaneous kinematic model is given by:

$$\dot{X} = J(q)\dot{q} \tag{9}$$

with $J(q) = \frac{\partial f}{\partial q}$.

We notice that generalized velocities $\dot{q}$ are dependent; they are linked by the nonholonomic constraint (Foulon et al. 1999).

The platform constraint described by equation (4) can be written in the following form:

$$[A(q_p) \;\; 0]\dot{q} = 0 \tag{10}$$

According to equation (5), the relation between the generalized velocities vector of the system and its control velocities can be written as:

$$\dot{q} = M(q)u = \begin{bmatrix} S_p(q_p) & 0 \\ 0 & I_n \end{bmatrix} u \tag{11}$$

where I_n is n order identity matrix and $u = [v, w, \dot{q}_{a1}, \cdots, \dot{q}_{an}]^T$.

The instantaneous kinematic model does not include the nonholonomic constraint of the platform given by equation (10).

The relation between the operational velocities of the mobile manipulator and its control velocities, which takes in account the nonholonomic constraint of the platform can be expressed by the instantaneous kinematic model (Bayle et al, 2001a.):

$$\dot{X} = \bar{J}(q)u \tag{12}$$

with $\bar{J}(q) = J(q)M(q)$.

3. Manipulability

3.1 Arm manipulator manipulability

One of the well-established tools for motion analysis of manipulator robot is the manipulability ellipsoid approach. Manipulability concept was originally introduced by Yoshikawa ((Yoshikawa, 1984), (Yoshikawa, 1985)) for manipulator arms to denote the measure for the ability of a manipulator to move

in certain directions. The set of all end-effector velocities that are realizable by joint velocities such that the Euclidean norm of $\dot{q}_a$, $\|\dot{q}_a\| = (\dot{q}_{a1}^2 + \dot{q}_{a2}^2 + \cdots \dot{q}_{an}^2)^{1/2}$, satisfies $\|\dot{q}_a\| \leq 1$, is an ellipsoid in m-dimensional Euclidean space. This ellipsoid represents an ability of manipulation. It is called the manipulability ellipsoid.
One of the representative measures of manipulation derived for the manipulability ellipsoid is

$$w = \sqrt{\det(J_a(q_a) J_a^T(q_a))} \tag{13}$$

In the case of non redundant manipulators ($n = m$), the measure w is reduced to

$$w = |\det(J_a)| \tag{14}$$

Manipulability has been utilized in many applications such as design, path planning and control of redundant manipulators. When the manipulator is redundant, there exists an infinity of solutions to the inverse kinematic. In this case, we need a criteria in order to extract a privileged solution. Sciavicco and Siciliano (Sciavicco, 1996) use the manipulability index as a criterion to be maximized to put the arm in a configuration far from its singular configurations and to ensure dexterous manipulation. Nakamura (Nakamura, 1991) and Yoshikawa ((Yoshikawa, 1990), (Yoshikawa, 1984)) further extend the redundancy exploitation with criteria expressed in Cartesian space: hence a secondary Cartesian task that can be satisfied without affecting the primary task. Simultaneous resolution of two tasks with different priorities is known as the *task priority strategy*.
In the field of mobile manipulators, Yamamoto (Yamamoto, 1987) has developed a control algorithm for mobile platform so that the manipulator arm is always positioned at the preferred configuration measured by its manipulability. A nonlinear feedback compensates the dynamic interaction between the mobile platform and the manipulator. Nagatani (Nagatani, 2002) has proposed an approach to plan mobile base's path which satisfies manipulator's manipulability. Controllers used for manipulation and locomotion are different.
Consider the singular value decomposition of J_a given by:

$$J_a = U_a \sum_a V_a^T \tag{15}$$

where $U_a \in R^{m \times m}$ and $V_a \in R^{n \times n}$ are orthogonal matrices and

$$\Sigma_a = \begin{bmatrix} \sigma_{a1} & & & 0 & \vdots & \\ & \sigma_{a2} & & & \vdots & \\ & & . & & \vdots & 0. \\ & & & . & \vdots & \\ 0 & & & \sigma_{am} & \vdots & \end{bmatrix} \in R^{m\times n}, \sigma_{a1} \geq \sigma_{a2} \geq \cdots \geq \sigma_{am} \qquad (16)$$

The manipulability measure *w* can be written as

$$w = \sigma_{a1} \cdot \sigma_{a2} \cdots \sigma_{am} \qquad (17)$$

In the literature, several other measures for kinematic manipulability have been given, among them:

$$w_2 = \frac{\sigma_{am}}{\sigma_{a1}} \qquad (18)$$

which gives the distance to singularities ((Lee, 1997), (Yoshikawa, 90)),

$$w_5 = \sqrt{1 - \frac{\sigma_{am}^2}{\sigma_{a1}^2}} \qquad (19)$$

which extends the notion of eccentricity of the ellipse (Bayle et al. 2001b), σ_{am}, σ_{a1} being respectively minimum and maximum singular values of J_a.

3.2 Mobile manipulator manipulability

Manipulability of mobile manipulator has been studied by few research groups. Yamamoto and Yun ([20]) have treated both locomotion and manipulation in the same framework from the viewpoint of task space. They present kinematic and dynamic contributions of manipulator and platform by the so called task space ellipsoid. Gardner and Velinsky (Gardner, 2001) have used the mobile manipulator manipulability in design purpose. The authors introduce numeric comparisons that allow to choose the position of a 3DOF anthropomorphic arm on the platform. Bayle et al. (Bayle et al., 2001a) have extended the definition of manipulability to nonholonomic mobile manipulators described by their reduced direct instantaneous kinematic models. The authors define a new measure w_5 and has been used it as a criterion to control mobile manipulators.

In the case of a mobile manipulator, the relation between the operational velocities $\dot{X}$ of the end-effector and the the velocity vector of the system

$u = [v, \omega, \dot{q}_{a1}, \cdots, \dot{q}_{an}]^T$ can be expressed by the reduced direct instantaneous kinematic model $\dot{X} = \bar{J}(q)u$.

$\dot{X}$ is expressed in m.s^{-1} while u is expressed in m.s^{-1} for the first linear velocity and in rad.s^{-1} for other ones. So coefficients of $\bar{J}$ have different units: no unit for the first column and meter for the last ones. This is an important difference with the case of the arm alone, in which all coefficients of J_a have the same unit. Moreover, with this formulation, preponderance risk of one of the subsystems (the platform or the arm) on the other is possible.

To solve this problem and to include the constraint on the maximum velocities of the system into manipulability, we propose to introduce the following normalized velocities in $\bar{J}$.

$$u_N = \left[\frac{v}{v_{\max}}, \frac{\omega}{\omega_{\max}}, \frac{\dot{q}_{a1}}{\dot{q}_{a1,\max}}, \cdots, \frac{\dot{q}_{an}}{\dot{q}_{an,\max}} \right]^T \tag{20}$$

Thus,

$$u_N = R^{-1}u \tag{21}$$

where

$$R = diag(v_{\max}, \omega_{\max}, \dot{q}_{a1,\max}, \cdots, \dot{q}_{an,\max}) \tag{22}$$

Note that *diag*(.) is diagonal matrix whose diagonal elements are specified by the arguments.

With these normalized control velocities, we can rearrange (12) as:

$$\dot{X} = \bar{J}(q)u = (\bar{J}(q)R)u_N = \bar{J}_N(q)u_N \tag{23}$$

With this new reduced Jacobian $\bar{J}_N$, we can define other manipulability measures.

$$\tilde{w} = \tilde{\sigma}_1\tilde{\sigma}_2\cdots\tilde{\sigma}_m \tag{24}$$

$$\tilde{w}_2 = \frac{\tilde{\sigma}_m}{\tilde{\sigma}_1} \tag{25}$$

$$\tilde{w}_5 = \sqrt{1 - \frac{\tilde{\sigma}_m^2}{\tilde{\sigma}_1^2}} \tag{26}$$

in which $\tilde{\sigma}_i$: are the singular values of $\bar{J}_N$, $1 \le i \le m$.

In the following section, we present simulation results for comparison of manipulability measures.

4. Comparison by simulation between measures

The structure of the manipulator arm consists in arm portion with three joints and wrist portion with three joints whose axes cross at one point. Indeed, it is interesting to divide the study into wrist and arm (the first three joint) singularities. This section presents the manipulability of the considered system for positioning tasks (arm portion). Subsection 4.1 presents analysis on manipulability measures of the arm alone and the mobile manipulator. After this analysis we will present in subsection 4.2 the application of manipulability concept to global control scheme to exploit the system redundancy.

4.1. Manipulability analysis

First, we analyze the manipulability of the arm for positioning tasks of the end-effector, then its extension to the case of the whole system (mobile manipulator). We show the influence of the presence of the mobile platform on measures.

4.1.1. Arm alone results

We consider a Manus arm for a positioning task (3DOF). We examine the evolution of manipulability for operational task which consists in following a straight line along x_{a1} from retracted configuration (point $(0, 0.12,0)^T$m) to extended one. Figure 3 shows the result obtained by the different manipulability measures presented in the previous section: w, w_2 and w_5.
Jacobian matrix of the manipulator arm for positioning tasks is depicted by:

$$J_a = \begin{bmatrix} -(L_4c_3 + L_3c_2)s_1 - L_2c_1 & -L_3c_1s_2 & -L_4c_1s_3 \\ (L_4c_3 + L_3c_2)c_1 - L_2s_1 & -L_3s_1s_2 & -L_4s_3s_1 \\ 0 & L_3c_2 & L_4c_3 \end{bmatrix} \quad (27)$$

where $c_i = \cos(q_{ai})$, $s_i = \sin(q_{ai})$ and L_2, L_3, L_4 represent the length of shoulder, upper arm and lower arm, respectively.
The joint velocity limits of the three links of the arm portion are the same. Thus, it is not necessary to normalize the Jacobian matrix.

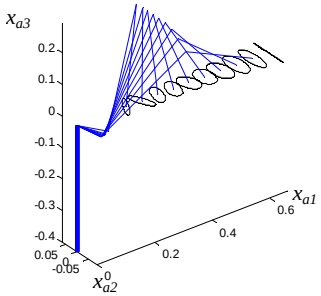

(a) Manipulability ellipses

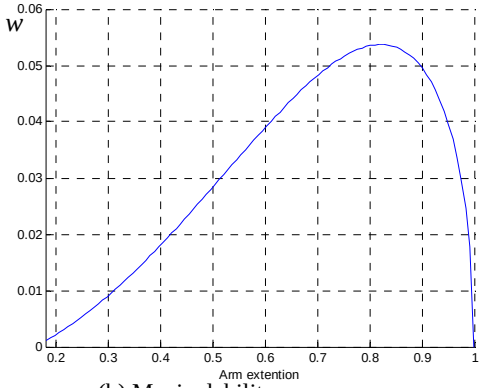

(b) Manipulability measure w

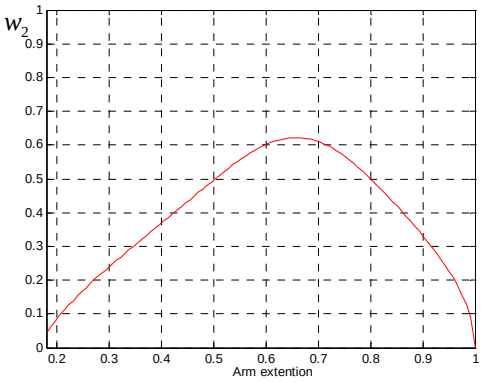

(c) Manipulability measure w_2

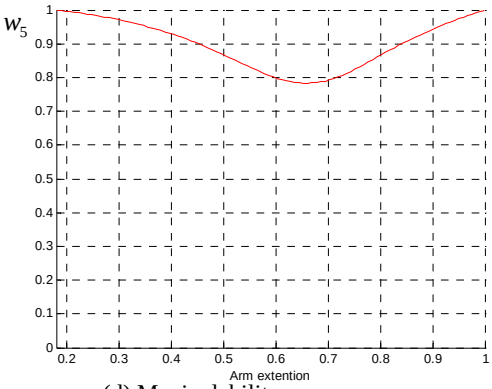

(d) Manipulability measure w_5

Arm extension: 0.2 folded up configuration – 1extended configuration.

Figure 5: Arm manipulability measures

Figure 5a shows the ellipses corresponding to the largest and the smallest singular values for certain configurations of the arm. Ellipse shapes give information about velocities distribution. Singular configurations correspond to a flat ellipse.

Figure 5b displays the evolution of the manipulability measure w. This measure takes into account all singular values of Jacobian matrix. It is equal to zero at singular values and increases when the arm reaches good configuration from manipulation point of view. Its value is proportional to the volume of the ellipsoid.

Like w, the manipulability measure w_2 (figure 5c) takes the value zero in singular configurations. It tends towards one when the arm moves away from its singularities.

Figure 5d displays the evolution of the manipulability w_5. It measures the ellipsoid eccentricity. When w_5 decreases to zero, possible end-effector velocities are becoming more isotropic and when w_5 tends towards one, the arm tends towards a singular configuration.

Discussion

Completely extended configuration of the arm corresponds to a singular configuration. Whatever, the manipulability measure used shows it. Manipulability indices w_2 and w_5 are more qualitative measures which provide the same information, but they evolve conversely. Indeed w_5 tends towards one for singular configurations whereas w_2 tends towards zero. In the following we will present only the two indices w and w_5.

The first axis of the arm manipulator does not possess joint limit, what permits to impose the same task in different direction of the operational space.

Figure 6 represents the shape the manipulability measures w and w_5 in the operational space when the x_{a3} is equal to zero. It shows that the manipulability of the manipulator arm does not depend on the orientation the first joint of the arm. Thus, for a given configuration (q_{a2}, q_{a3}) of the arm, manipulation abilities are the same whatever direction of the operational space.

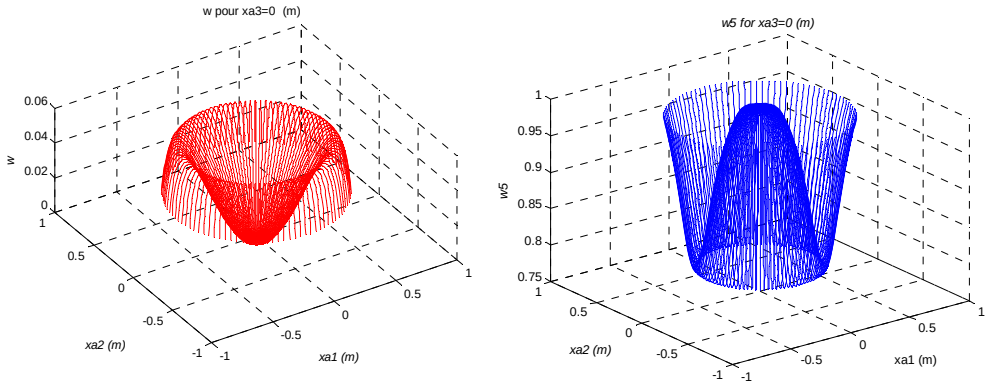

Figure 6: Distribution of the manipulability in the XY

4.1.2. Mobile arm results

Now, we consider Manus arm mounted on the mobile platform. The arm base is in the middle of the wheels axis (a=b=0). We use the same simulation setting as in previous example (same imposed task to end-effector). For this task, the platform does not move, but its capacity to move is taken into account in the computation of manipulability.

The reduced Jacobian matrix of the mobile arm is given by:

$$\bar{J}(q) = \begin{bmatrix} c_{\theta_b} & \bar{J}_{12} & \bar{J}_{13} & \bar{J}_{14} & \bar{J}_{15} \\ s_{\theta_b} & \bar{J}_{22} & \bar{J}_{23} & \bar{J}_{24} & \bar{J}_{25} \\ 0 & 0 & J_{a31} & J_{a32} & J_{a33} \end{bmatrix} \tag{28}$$

where

$$c_{\theta_p} = \cos(\theta_p), \quad s_{\theta_p} = \sin(\theta_p)$$

$J_{aij} = J_a(i, j)$ given by equation (27)

$$\bar{J}_{12} = -(x_{a2} + a)s_{\theta_p} - (b - x_{a1})c_{\theta_p},\ \bar{J}_{13} = J_{a21}c_{\theta_p} + J_{a11}s_{\theta_p}$$

$$\bar{J}_{14} = J_{a22}c_{\theta_p} + J_{a12}s_{\theta_p},\ \bar{J}_{15} = J_{a23}c_{\theta_p} + J_{a13}s_{\theta_p},$$

$$\bar{J}_{22} = (x_{a2} + a)c_{\theta_p} - (b - x_{a1})s_{\theta_p},\ \bar{J}_{23} = J_{a21}s_{\theta_p} - J_{a11}c_{\theta_p},$$

$$\bar{J}_{24} = J_{a22}s_{\theta_p} - J_{a12}c_{\theta_p},\ \bar{J}_{25} = J_{a23}s_{\theta_p} - J_{a13}c_{\theta_p}.$$

To illustrate the importance of the normalization proposed in section 3.2, we present results obtained with the manipulability measure w_5. Then, we give results obtained with the new normalized measure $\tilde{w}_5$. In our case, normalization does not bring anything for w measure.

First, evolution of manipulability measure w_5 of the mobile manipulator is displayed in figure 7a. In this case, arm end-effector motion is perpendicular to mobile platform displacement. Measure has globally the same shape as in the case of the arm alone. When the arm is extended, the configuration of the whole system is singular: values of w_5 are close to one. Thus, the global system is far from its isotropic configurations. Figure 7b shows the same measure, but now the end-effector task is to follow a straight line parallel to mobile platform displacement. When the arm is extended, the configuration of the whole system is not more singular: value of w_5 becomes less than one. Indeed, the platform effect on the whole system manipulability is dominant and does not reflect the real case.

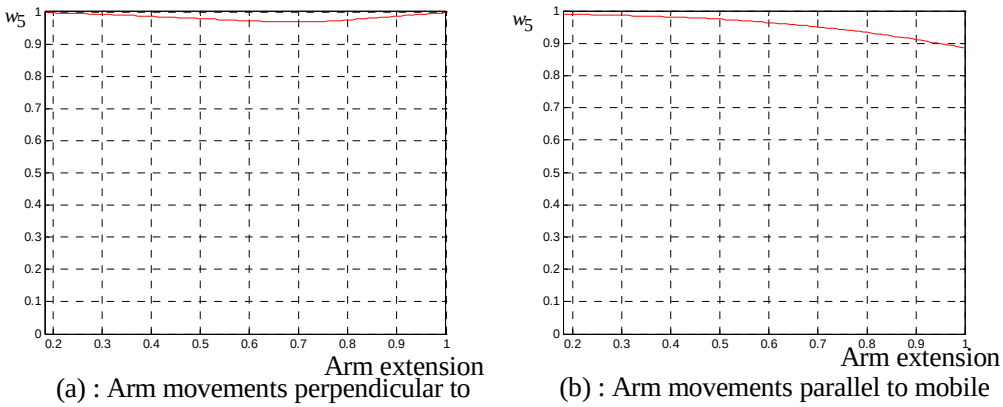

(a) : Arm movements perpendicular to mobile platform displacement

(b) : Arm movements parallel to mobile platform displacement

Figure 7: Manipulability of the mobile manipulator

We present now the simulation results after normalization. The maximum of the system velocities are fixed to:

$$u_{\max} = \left[0.33, 0.55, \frac{\pi}{3}, \frac{\pi}{3}, \frac{\pi}{3}\right]^T \text{(m.s}^{-1}\text{, rad.s}^{-1}\text{, rad.s}^{-1}\text{, rad.s}^{-1}\text{, rad.s}^{-1}\text{)}$$

Figure 8a displays the evolution of manipulability $\tilde{w}_5$ of the mobile arm. Figure shows that mobile manipulator manipulability shapes are the same as for the arm alone, and singular configurations remain the same. The mobile platform cannot instantaneously move in direction perpendicular to its main axis because of the nonholonomic constraint. Therefore, the manipulability of the whole system is reduced to the one of the arm. Figure 8b shows the evolution of the manipulability $\tilde{w}_5$ of the mobile manipulator for the same task, but now the motion is along x_{a2} which corresponds to longitudinal axis of the mobile platform. The effects of the mobile platform on the shape of ellipsoid and manipulability measure are relevant. Like for w_5, extended arm configuration becomes non singular for the global system. But extended configuration of the arm does not give the best value of $\tilde{w}_5$.

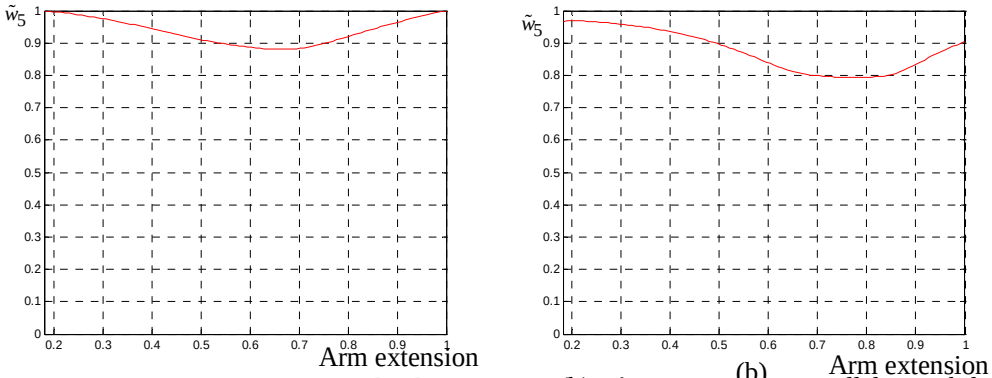

(a) : Arm movements perpendicular to mobile platform displacement

(b) : Arm movements parallel to mobile platform displacement

Figure 8: Normalized measures of the mobile manipulator manipulability

Discussion

We presented the extension of manipulability concept to the case of mobile manipulators which have a more complex structure than a simple manipulator arm. Manipulability of the mobile manipulator takes into account of contribution of each part of the system i.e. platform and manipulator arm.

Mobile manipulator manipulability measures w and w_5 as defined do not take in consideration real limits of the system. Normalized measures which we have proposed allow to include maximum values of the system velocities into the manipulability and to solve problems inherent to physical units.

Mobile manipulator manipulability w_5 evolution (figure 7b) shows that completely extended configuration of the arm which is singular corresponds to the best one for the mobile manipulator. Whereas, normalized measure $\tilde{w}_5$ (figure 8b) which takes into account the velocity limits, shows a deterioration of the measure for this configuration what better reflects reality. Thus, it is interesting to use the normalized measures $\tilde{w}_5$.

Moreover, this measure is optimized when arm configuration is far from its completely extended one.

4.2. Application of the manipulability in mobile arm control

The redundancy of mobile manipulators plays an important role increasing their flexibility and versatility. Based on manipulability measures, a control algorithm for utilizing the redundancy for singularity avoidance is given in subsection 4.2.1. Subsection 4.2.2 shows simulation results on the considered system.

4.2.1 Inversion scheme

There are many mapping techniques for resolving the redundancy of the combined system (mobile manipulator). The pseudo inverse of the matrix $\overline{J}$ is:

$$\overline{J}^{+} = \overline{J}^{T}(\overline{J}\overline{J}^{T})^{-1} \tag{29}$$

will provide the minimum norm of the control velocities. By adding the null-space projector to equation we get (Bayle et al., 2001b)

$$u = \overline{J}^{+}\dot{X}_{d} - (I_{N-1} - \overline{J}^{+}\overline{J})W(\frac{\partial P}{\partial q}M)^{T} \tag{30}$$

in which $\dot{X}_{d}$ is the vector of desired task, W is a positive weighting matrix , M is given by (11) and $P(q)$ is the objective function depending on the configuration of the manipulator arm.

The first term in this equation is the particular solution of the system while the second one is the homogeneous solution and provides no motion of end-effector (Baerlocher, 2001). The choice of the function to be optimized can be the manipulability of the arm or that of the whole system. To ensure dexterous manipulation, it is interesting to put the arm in a configuration far from its singular configurations. In the following, we present simulation results obtained without any optimization, then by optimizing manipulability measures w_5 of both arm and mobile arm, and the normalized measure $\tilde{w}_5$ of mobile arm.

4.2.2 Simulation results

In this section, we consider a Manus arm mounted on a nonholonomic mobile platform powered by two independent drive wheels. The mobile platform is initially directed toward positive X_W-axis at rest (q_p=[0 0 0]^{T}) and the initial configuration of the manipulator arm is q_a=[$\frac{\pi}{2}$; $\frac{\pi}{3}$; $-\frac{\pi}{3}$].

Two different paths of end-effector are used for the simulation. Velocity along a path is constant and equal to 0.05m.s^{-1}. There are two imposed tasks.

Case 1: following a straight line along the X_W-axis of the world frame $\{W\}$.

Case 2: following a straight line along the Y_W-axis of the world frame $\{W\}$.

The initial coordinates of arm base with respect to the world frame are (0.12, 0.12, 0.4) m. For each simulation, we plot the manipulability measure of the arm, the end-effector and platform axis middle point trajectories.

To avoid confusion between manipulability measures of the arm and the mobile manipulator, we note in the sequel w_{a5} the measure related to the arm.

We report results obtained in the following cases:

- Without any optimisation, by using only pseudo inverse formulation which gives minimum norm solution for control velocities.
- Optimizing manipulability measure w_{a5} of the arm.
- Optimizing manipulability measure w_5 of the mobile manipulator.
- Optimizing normalized measure $\tilde{w}_5$ of the mobile manipulator.

Case1: following a straight line along platform displacement.

We firstly present on figure 9 results obtained without any criterion optimization, by using only the pseudo inverse $u = \overline{J}(q)\dot{X}_d$ which is a particular solution. The manipulator arm and the platform move simultaneously to carry out the imposed task. Figure 9a shows the arm manipulability measure w_{a5} which improves in the beginning then deteriorates to take the value one which is a singular configuration. Manipulator arm evolves from initial configuration toward its extended one. Figure 9b displays the end-effector and platform middle wheels point trajectories.

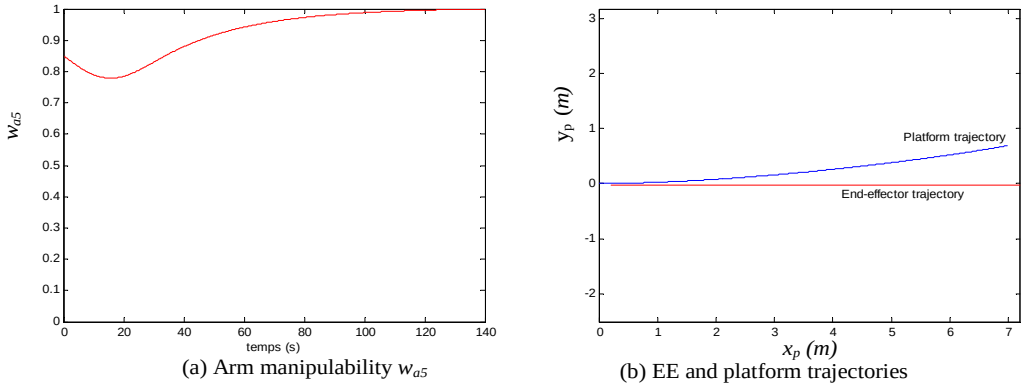

(a) Arm manipulability w_{a5} (b) EE and platform trajectories

Figure 9: simulation result without optimizing any criterion

Figure 10 shows the execution of the same task by optimizing the manipulability criterion w_{a5} of the manipulator arm alone. This measure equal to one at singular configurations. The evolution of the manipulability measure w_{a5} represented in figure 10a tends to improve quickly, reaches its minimum (better configuration) and stabilizes into the neighbourhood of this value. As shown on figure 10b, end-

effector follows correctly the trajectory. The platform moves back for short distance to contribute in manipulability improvement, and moves forward after this transient state.

Once the arm reaches its best posture, the remaining part displacement is carried out by the platform.

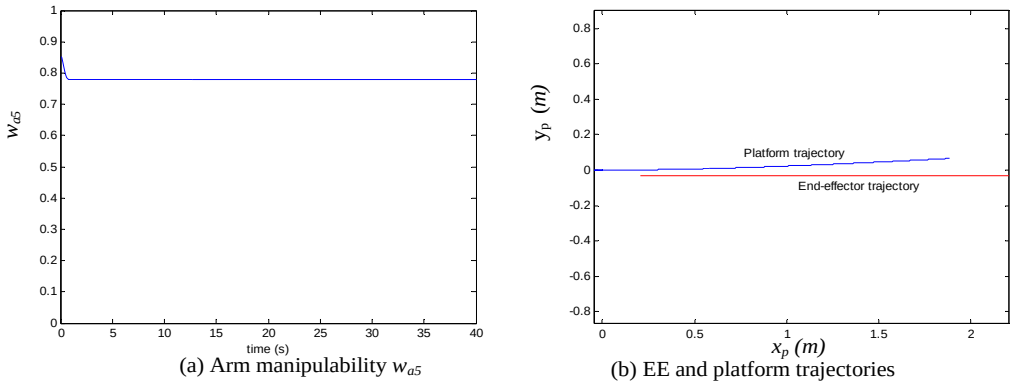

(a) Arm manipulability w_{a5} (b) EE and platform trajectories

Figure 10 : simulation result with optimizing the manipulability measure w_{a5} of the arm

Figure 11a gives the evolution of manipulability measures w_{a5} of the arm and w_5 of the mobile when this last measure is optimized. It is seen that the manipulability w_5 of the mobile arm improves quickly, whereas the arm one deteriorates (takes the value 1), because arm reaches its extended configuration. On figure 11b are given the trajectories of the end-effector and the platform. It is noticed that the platform moves almost in straight line. At the beginning, the platform moves back a little in straight line to contribute to the minimization of the considered measure. At the same time, the arm modifies its configurations to optimize w_5. However w_{a5} is not optimized which corresponds to arm singular configurations.

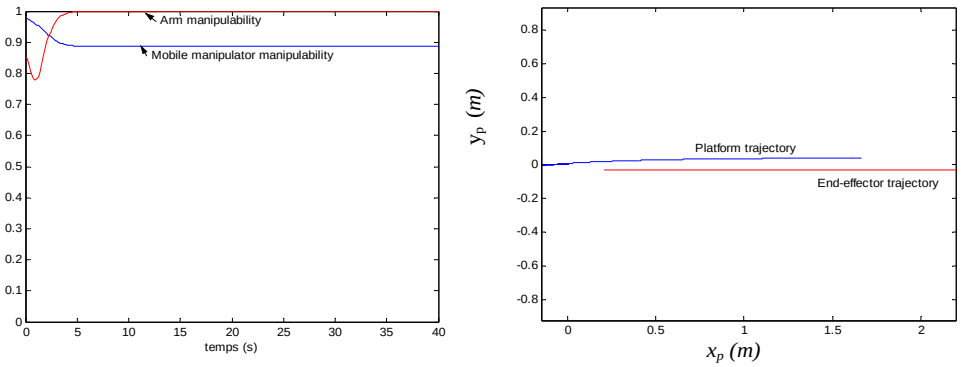

(a) Manipulability measures w_{a5}, w_5 (b) EE and platform trajectories

Figure 11: simulation result with optimizing the manipulability measure w_5 of the mobile arm

As waited in 3.2, optimizing the mobile manipulator manipulability measure $\tilde{w}_5$ allows to makes it possible to reinforce the influence of the arm. Indeed, figure 12a shows that w_{a5} is less than one (far from singular configuration) although the optimization is calculated on the whole system. Figure 12b shows that end-effector trajectory is correctly executed and platform follows almost a straight line.

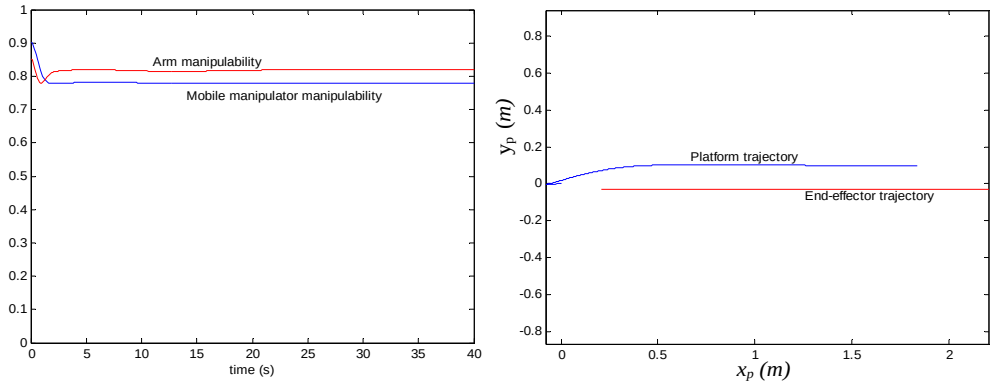

(a) Manipulability measures w_{a5}, $\tilde{w}_5$

(b) EE and platform trajectories

Figure 12: simulation result with optimizing the manipulability measure $\tilde{w}_5$ of the mobile arm

Case2: following a straight line perpendicular to platform displacement.

Figure 13 shows the simulation result obtained by the pseudo inverse scheme $u = \bar{J}(q)\dot{X}_d$ without using any performance criterion. The arm evolves from its initial configuration to its extended one while passing by configurations indicating a good measure of manipulability. The arm reaches a singular configuration after 20 seconds. As depicted in figure 13b, the platform is initially badly directed with respect to task direction and its contribution is limited by the nonholonomic constraint. To carry out the desired task, the platform is constrained to change its direction of motion. However, the mobile arm achieves the imposed task with bad arm configuration from arm manipulation point of view.

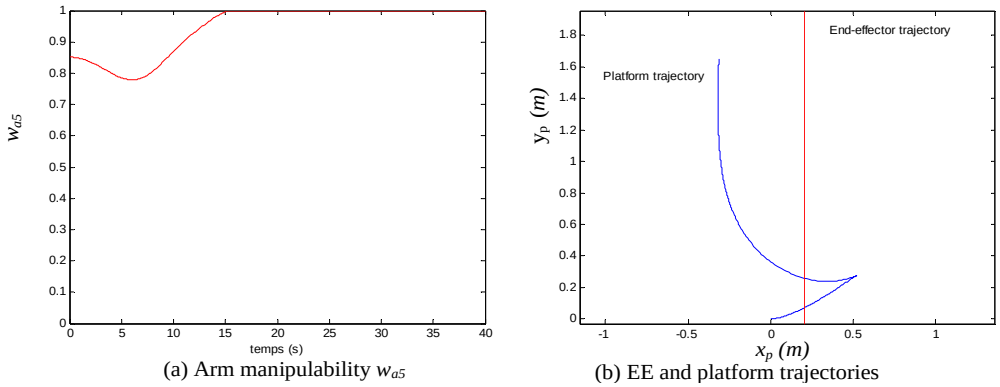

(a) Arm manipulability w_{a5} (b) EE and platform trajectories

Figure 13: simulation result without optimizing any criterion

Figure 14 shows the simulation results when the arm manipulability w_{a5} is used as performance criterion to solve the redundancy of the mobile arm. As depicted in figure 14a, the arm manipulability w_{a5} quickly improves which implies that the arm evolves toward a good configuration from point of view of optimized measure.

The arm is initially in a configuration corresponding to a bad manipulability. To improve quickly the manipulability of the arm while carrying out the imposed task, the arm extends and the platform moves back (figure 14b). The platform stops moving back once the manipulability of the arm is optimized, then it advances so that the set carries out the imposed task. This evolution corresponds to the first graining of the trajectory of the platform. As the platform is badly directed with respect to the task direction, its contribution is limited by the nonholonomic constraint. That causes a temporary degradation of the manipulability shown in figure 14a. The reorientation of the platform, which corresponds to the second point of graining, allows the optimization of w_{a5}.

The mobile arm achieves the desired task with good configuration for the arm from manipulation point of view and the platform takes a good orientation after two changes of directions.

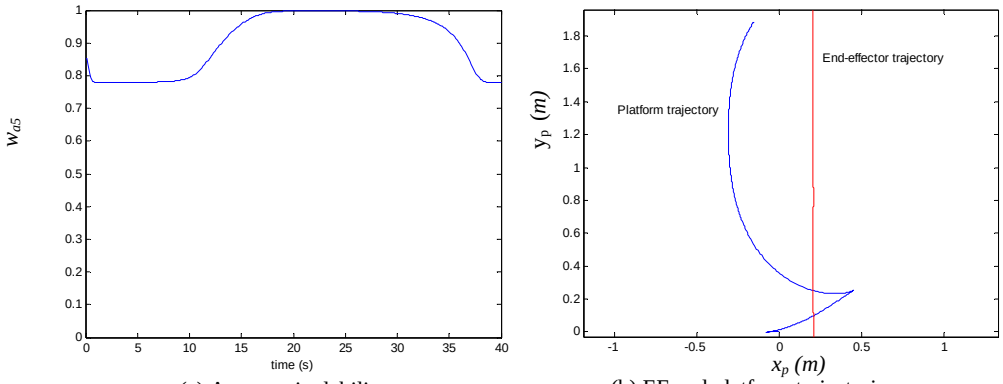

(a) Arm manipulability w_{a5} (b) EE and platform trajectories

Figure 14: simulation result with optimizing the manipulability measure w_{a5} of the arm

Figure 15 displays results obtained when the mobile manipulator manipulability w_5 is optimized. Figure 15a gives the evolution of the manipulability measures w_{a5} of the arm and w_5 of the mobile arm. It is seen that the manipulability w_5 of the mobile arm improves quickly, whereas the arm measure increases up to one, because the arm reaches its extended configurations. Configurations which optimize the manipulability measure w_5 of the whole system are bad ones for the arm. Figure15b shows that end-effector trajectory is correctly executed. The platform moves back at beginning, which corresponds to improvement of the manipulability measures w_{a5} and w_5. The motion of the platform and the arm is coordinated to carry out the imposed task. Arm reaches extended configurations which optimize the measure w_5, but not w_{a5} as seen in case 1.

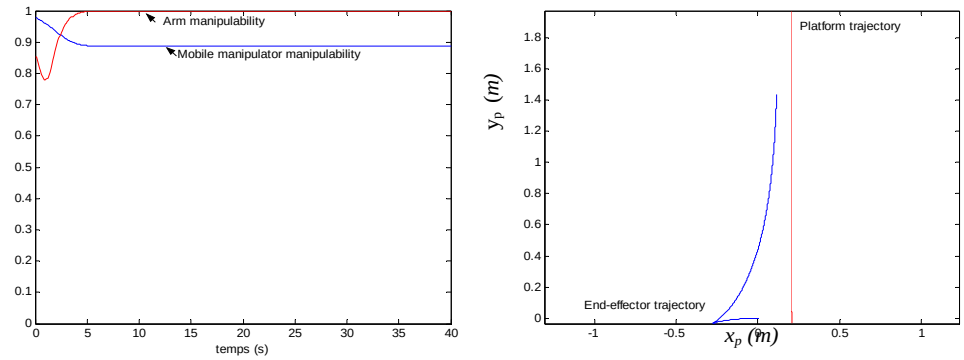

(a) Manipulability measures w_{a5}, w_5 (b) EE and platform trajectories

Figure 15: simulation result with optimizing the manipulability measure w_5 of the mobile arm

Figure 16 shows the case of optimizing performance criterion related to the normalized mobile manipulator manipulability measure $\tilde{w}_5$. Both mobile manipulator and arm manipulability measures $\tilde{w}_5$ are shown in figure 16a. The

corresponding arm configurations are good from arm manipulability point of view, measured by w_{a5}.

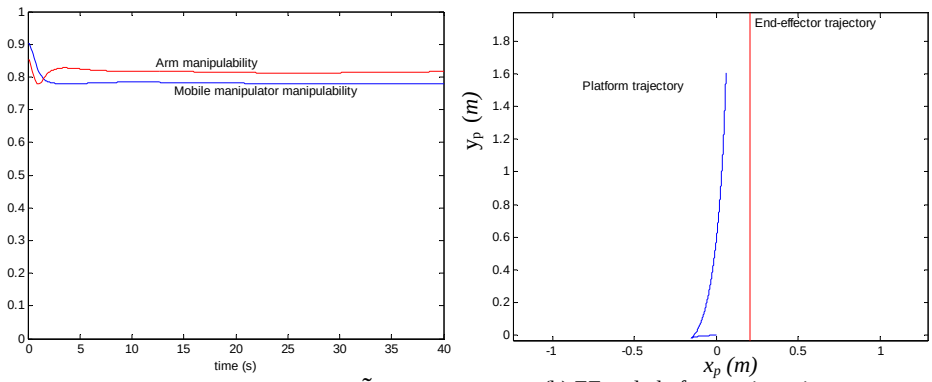

(a) Manipulability measures w_{a5}, $\tilde{w}_5$ (b) EE and platform trajectories

Figure 16 : simulation result with optimizing the manipulability measure $\tilde{w}_5$ of the mobile arm

4.2.3 Discussion

The purpose of this study is to exploit the redundancy generated by association of the manipulator arm and the mobile platform in order to put the manipulator arm in good configurations from manipulation point of view and to reduce energy consumption during the task execution i.e. to have smooth movements. The measure used to characterise arm manipulation ability is w_{a5}. In our case, arm manipulation ability is satisfying when w_{a5} <0.9. For energy consumption, the idea is to reduce strong acceleration variations by limiting platform manoeuvres number. The number of trajectory grainings is a good indicator.

Pseudo inverse is a particular solution which gives the minimum velocities of the system to execute the operational task. Whatever the task, arm configurations obtained by this solution (figure 9 and 13) are not optimized from manipulation ability point of view. Platform trajectories are not constrained by arm configurations but only depend on the task to be carried. So, we have introduced criterion optimization for controlling the system.

To guaranty the first objective, arm manipulability measure w_{a5} is optimized for controlling the whole system. By construction, the arm adopts configurations well-adapted to manipulation tasks. Platform trajectory is smooth in the case of following a straight line along platform displacement (case1, figure 10), whereas two changes of direction (graining points) appear in following a straight line perpendicular to platform displacement (case2, figure 14). The use of the global criterion w_5 should limit the number of manoeuvres. Optimizing the mobile

manipulator manipulability measures allows taking into account mobility capacities offered by the mobile platform. Figure 15b shows only one graining in platform trajectory. Therefore, figures 11a and 15a show that w_{a5} close to 1. Indeed, the arm is completely extended because the influence of platform is dominating with regard to the arm. The optimizing of the normalized measure $\tilde{w}_5$, which takes into account the velocity limits of the system, allows the balance of influence of both parts of the global system. Arm configurations are generally far from its extended ones in the opposite of the case of optimizing w_5. Platform trajectories are globally smooth with a weak graining at beginning (figure 12 and 17).

5. Conclusion

In the field of disabled people assistance, the objective of this work is to give to disabled operators the possibility to pilot a mobile arm which is a manipulator arm mounted on a mobile base. Main missions are "go and take back an object" and "manipulate an object". The spot of this paper is to exploit redundancy of the system to maximise the manipulability of the arm and, if possible, to minimise the energy necessary to reach the goal fixed by the user. This last criterion is based on human strategies studied for the same kind of tasks. Several measures of manipulability have been compared, taking into account the arm alone or the global system. Several of them come from literature. In the case of the global system, a new criterion has been proposed in order to give an equal weight to both manipulator arm and mobile base. With regard to the arm alone, all three criteria provide information on the arm capacity to move, depending on its extension. However w_2 and w_5 are very similar in their form and do not provide additional information about manipulability. With regard to the global system the most interesting result, based on w and w_5 criteria, comes from the normalisation proposed. In the case of w_5, the normalised version of the criterion permits to have a good appreciation of the movement capacity of the arm while w_5 can not. Neither w nor its normalised version provide this information.
Manipulability criteria have also been used to control the system. In that case, a comparison has been made between command using criteria minimisation and command without minimisation, the latter is taken as reference. The main result is that using the normalised version of the criterion w_5, acceleration variations

decrease and trajectories become smoother so expenditure of energy is reduced. This can be shown by analysing the trajectory followed by the mobile platform. w and w_5 provide trajectories with two graining points and w_5 provides a trajectory with only one graining point. Results presented here show that our criterion permits to have a satisfying control of the global system, taking into account manipulability and energy. Present works try to improve the criterion taking into account the task to be realised. Indeed, manipulability giving information on the capacity of the system to move, the idea is to measure this capacity taking into account the privileged direction of the task. This will permit to obtain a more precise criterion and to elaborate a better command of the system.

References

1. Alexander, R.McN.: A minimum energy cost hypothesis for human arm trajectories, Biological Cybernetics, 1997, Vol. 76, n°2, pp.97-105.

2. Baerlocher, P.: Inverse kinematics techniques for the interactive posture control of articulated figures, PhD thesis, Lausanne, EPFL 2001.

3. Bayle, B., Fourquet, J.Y. and Renaud, M.: Using manipulability with nonholonomic mobile manipulators, Int. Conf on Field and Service Robotics, Helsinki, Finland, June 2001, pp.343-348.

4. Bayle, B., Fourquet, J.Y. and Renaud, M.: Manipulability Analysis for Mobile Manipulators, In ICRA'2001, Séoul, South Korea, May 2001, pp. 1251-1256.

5. Fong, T., and Thorpe, C.: Vehicle teleoperation interface. *Autonomous Robots*, 2001, *11*, 9-18.

6. Foulon, G., Fourquet, J.Y. and Renaud, M.: Coordinating mobility and manipulation using nonholonomic mobile manipulators, In ISER'99, Sydeny. Australia, March 1999, pages 115-125.

7. Gardner, J. and Velinsky, S. : Kinematics of Mobile Manipulators and implications for Design, Journal of Robotic Systems, 2000, Vol.17, n°6. pp. 309-320.

8. Hoppenot, P., Colle, E.: Mobile robot command by man-machine co-operation - Application to disabled and elderly people assistance, Journal of Intelligent and Robotic Systems, July 2002, vol. 34, n°3, pp. 235-252.

9. LEE, J.: A study on the manipulability measures for robot manipulators, IROS1997, France, Grenoble, September1997, pp. 1458-1465.

10. Mestre, D.R., Rybarczyk, Y., Hoppenot, P., Colle, E : Assistance Robotics: Implementation of human-like visuo-motor synergies on a teleoperated mobile device, CSUN's 20th Annual International Conference Technology and Persons with Disabilities, March 14-19, 2005 ~ Los Angeles, CA

11. Nagatani, K. Hirayama, T. Gofuku, A., Tanaka, Y.: motion planning for mobile Manipulator with keeping Manipulability, IROS 2002, Lausane, Switzerland, October 2002, pp 1663-1668.

12. Nakamura, Y.:Advanced robotics, redundancy and optimization, Addison Wesley Publishing, 1991.

13. Rybarczyk, Y., Etienne, C., Hoppenot, P.:Contribution of neuroscience to the teleoperation of rehabilitation robot, - SMC'2002, Hammanet, Tunisia, abstract p.75, 6-9 October 2002

14. Rybarczyk, Y., Galerne, S., Hoppenot, P. Colle, C., Mestre, D. : The development of robot human-like behaviour for an efficient human-machine co-operation, AAATE, Ljubjana, September 2001, pp.274-279,3-6.

15. Sciavicco, L. and Siciliano, B.: Modeling and control of robot manipulators, The McGraw-Hill companies, inc., 1996.

16. Seraji, H.:An on-line approach to coordinated mobility and manipulation., In *ICRA'1993*, Atlanta, USA, may 1993, pp. 28-35
17. Yamamoto, Y. and Yun, X.: Unified analysis an mobility and manipulability of mobile manipulators, IEEE Int. Conf. Robotics and Automation, Detroit, USA, 1999, pp. 1200-1206.
18. Yamamoto, Y. and Yun, X.: Coordinating locomoation and manipulation of mobile manipulator, Recent Trends in Mobile Robots Zheng Y. Ed., 1987.
19. Yoshikawa, T.: Foundation of robotics: Analysis and control, The MIT Press, 1990.
20. Yoshikawa, T.: Manipulability of Robotic Mechanisms, International Journal of Robotics Research, 1985, vol. 4, n° 2, pages 3-9.
21. Yoshikawa, T.: Analysis and control of Robot manipulators with redundancy, In M. Brady & R. Paul, editeurs, Robotics Research: The First International Symposium, MIT Press, 1984, pages 735-747.